ChemComm

Accepted Manuscript

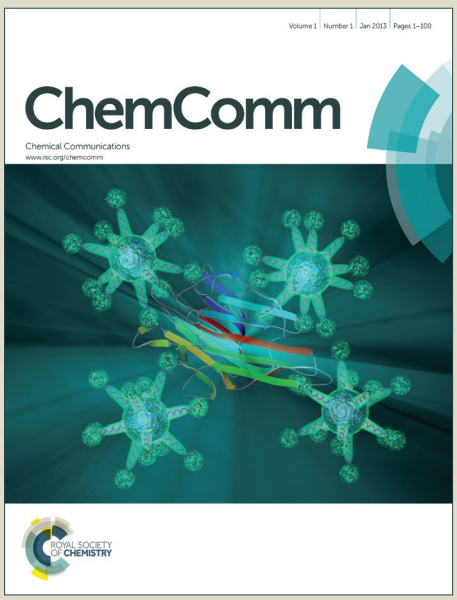

ROYAL SOCIETY OF CHEMISTRY

www.rsc.org/chemcomm

Journal Name

RSCPublishing

COMMUNICATION

Rapid, High Yield, Directed Addition of Quantum Dots onto Surface Bound Linear DNA Origami Arrays†

Cite this: DOI: 10.1039/x0xx00000x

Masudur Rahman*, David Neff and Michael L. Norton

Received 00th January 2012,
Accepted 00th January 2012

DOI: 10.1039/x0xx00000x

www.rsc.org/

We have developed an approach, which routinely generates ~10 micron long one dimensional (1D) arrays of DNA origami. Coupled with a sequential assembly method with a very short (~1 min.) reaction time, this extended platform enables the production, in high yield, of 1D arrays of biomolecules or conjugates.

The objective of nanotechnology is to organize matter with the highest precision and control, which will lead to advances in many fields, including nanoelectronics, nanorobotics and nanoscale signal transducers. Structural DNA nanotechnology has great potential to enable these advances.[1-3] Among the many demonstrations of the use of DNA as a building block material for the construction of nanostructures are DNA origami,[4, 5] rafts,[2, 6, 7] and DNA octahedra.[8]

DNA origami (DO) can themselves be assembled into larger structures[5, 9, 10] extending their potential for small-scale device applications.[11-13] Many researchers have reported the generation of 1D and 2D origami arrays by attaching individual origami;[9, 10, 14-16] however the array formation yield and extent (dimensions) require improvement.[17] Although current sizes are large enough to connect bottom-up methods of patterning with top-down approaches, even larger scales will enable manufacturing breakthroughs, particularly if coupled with indexed localization within arrays.

Therefore we have designed and fabricated one dimentional rectangular DNA origami (1DrDO) to partially address this barrier. In this paper implementation and characterization of a simple and very rapid labeling method for directing Streptavidin (SA) or SA coated Quantum Dots (SA-QDs) to specific locations on single rectangular DNA origami (srDO) and 1DrDO with high yield is described. The molecular combing methods[18, 19] was used to align partially immobilized SA-QD labeled 1DrDO complexes in one direction on APTES coated glass coverslips (AP-glass). Linearizing the arrays via the combing technique enhances the potential value of one dimensional origami arrays for analytical applications.

Department of Chemistry, Marshall University, West Virginia 25755 USA
**Email: rahmanm@marshall.edu; Tel: 1-304-696-3569; Fax: 1-304-696-3243*
†Electronic Supplementary Information (ESI) available: Experimental details and Figures S1−S12. See DOI: 10.1039/c000000x/

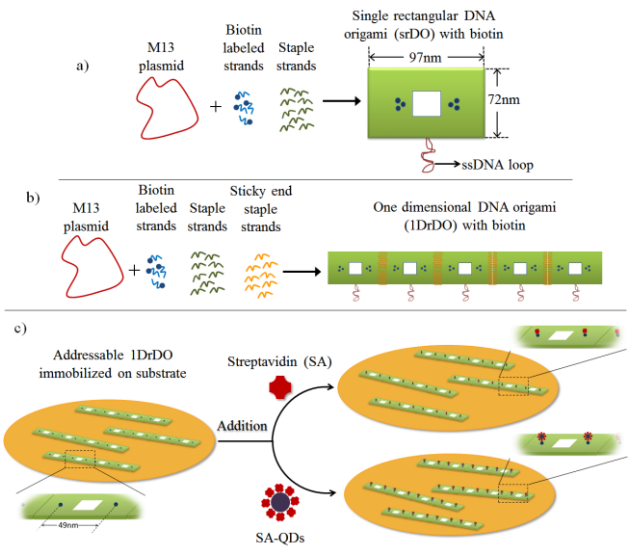

Figure 1. Schematic illustration representing a) self-assembly of m13 plasmid, biotin (blue) labeled strands and staple strands (deep green) to form rectangular shaped biontinylated DNA origami (srDO, green); b) represents self-assembly of one dimensional rectangular origami (1DrDO) with the help of sticky end staple strands (orange); c) illustrates the addition of streptavidin (SA, red) or SA-QDs (purple-red) onto surface bound biontinylated 1DrDO.

DNA origami platforms:

M13mp18 ssDNA plasmid (7249bp), short complimentary DNA staple strands, and biotin labeled strands were used to program the rectangular shaped origami platforms. The form of the 97 nm×72 nm srDO with a 22 nm×26 nm landmark window in the center is illustrated in Fig. 1a. This origami design scaffold does not use 1480bp of the ssDNA plasmid. This remaining ssDNA forms an identifiable loop on one of the long edges of the srDO construct (Fig 1a). The design of the 1DrDO, includes complementary sticky end staples (optimized sequences provided in ESI) along the short edges

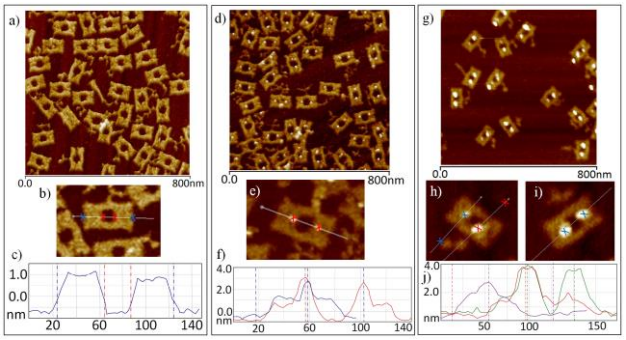

Figure 2. AFM images show the srDO on mica and addressing of SA and SA-QDs onto srDO; a) single rectangular origami (srDO) on mica, b) and c) show high resolution srDO and cross section respectively; d) two SA addressed onto srDO; e) and f) high resolution and line profile showing SA labeling characteristics; g) SA-QDs addressed onto srDO; h) srDO labeled with two SA-QDs; i) srDO labeled with SA and SA-QD; j) composite line profile comparing the height of modifications on labeled srDO.

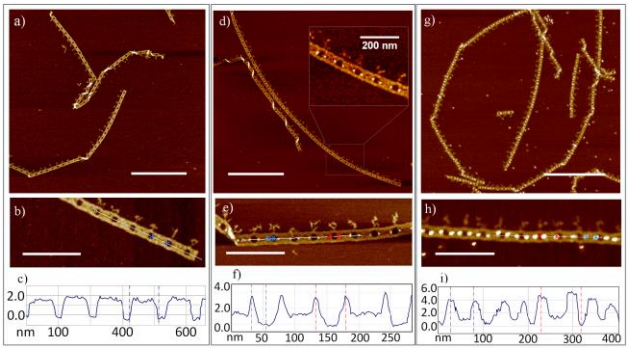

Figure 3. Figure 3: AFM images show the addressing of SA and SA-QDs onto 1DrDO; a) long 1DrDO on mica, (b) high resolution and (c) line profile indicating the window pitch of 1DrDO; d) SA modified long 1DrDO, inset shows magnified image (e) high resolution shows the high yield of SA modification and (f) line profile, which indicates the height of SA on origami; g) SA-QD modified 1DrDO; h) high resolution and i) line profile reflecting variations in SA-QD labeling; Scale bar 1μm

of the srDOs such that the single DO bind each other only in one orientation, as illustrated in Fig. 1b. The low magnification AFM image in ESI Fig. S4 indicates the high yield of extended 1DrDO structures.

SA or SA-QDs modification of immobilized srDO constructs:

Two sites on the srDO constructs were coded for addressing SA or SA-QDs by adding three biotin labeled strands complementary to the M13 plasmid at each site on the DO platform. At each site, the three biotins were positioned with ~2nm spacing in a triangular configuration, as schematized in Fig. 1a. ESI Fig. S12 indicates in greater detail the locations of the biontinylated staples. Hendrickson *et al.* reported that the tetrameric strepta7vidin structure has four identical β-barrels with the biotin binding-sites located at one end of each barrel, which are 2 nm apart.[20] Therefore, the three biotins on each side of the origami can bind at least one SA, optimally via 3 of its 4 "ports". Fig. 1c depicts a schematic diagram of a biotinylated 1DrDO with two blue dots that represent the two groups of biotins located at a separation distance of 49 nm. A representative AFM topography image (Fig. 2a) and analysis (Figs. 2b,c) of srDO immobilized on mica before incubation with SA can be compared with Fig. 2d,e and f, which show different regions of the same sample after being successfully modified with SA. Here origami was immobilized first on mica, modified by 1 minute of directed assembly, then rinsed. The line profile analysis of Fig. 2a reveals that the two modifications (Fig.2f) were separated by 44±3nm (*N*=134, number of origami counted) and on average these modifications are 3.4±0.5 nm (*N*=134) in height (3.4 nm is the sum of the heights of SA and the DNA origami. The height of SA is ~2.4 nm as the DNA origami height is determined to be ~1.1nm in Fig. 2c). The spacing is consistent with the designed biotin locations on srDO and the observed SA height is consistent with other reported observations of SA on origami.[21] These modifications lead to SA being addressed with a yield of ~99% (*N*=273, Table 1 in ESI). Figure 1c presents a high-resolution AFM image of SA-QDs, which have been addressed to specific locations on srDO. In this case, the origami were also immobilized first on mica and then interacted with a SA-QD solution. High-resolution AFM images of this labeling are shown in Fig. 2h and 2i. Line profile analysis indicated that both attached particles in Fig. 2h are ~5.5 nm in height, whereas in Fig. 2i one particle measures around ~2.6nm and the other one is ~5.5nm in height. It is reasonable to conclude that the particles with the higher elevation (~5.5 nm) are SA-QDs (5.5 nm is the sum of SA-QDs and DO's height. The height of SA-QDs is ~4.5 nm as the DO height indicated in Fig. 2c is ~1nm). Purchased SA-QDs were used here without any further purification, with yield falling with increasing age of the SA-QD assemblies. SA apparently dissociates from the SA-QD conjugate, resulting in the observed SA blocked attachment sites. Although significant (12%) miss-attachment was observed, 77% (*N*=341) of the srDO were labeled with two SA-QD and could be considered satisfactory for prototyping applications.

SA or SA-QD modification of immobilized 1DrDO constructs:

The rigidity of 1D origami is sufficiently great to enable the alignment of species in a periodic pattern over relatively long distances. Having demonstrated success in addressing SA or SA-QDs to binding sites at fixed distances on srDO, the same technique was implemented with 1DrDO as illustrated in Fig. 1C. Arrays of this origami, periodically presenting biotin binding locations along the midline region of the 1DrDO constructs, is shown schematically in Fig.1b. The AFM image in Fig. 3a presents examples of long 1DrDO constructs which were successfully formed in solution then immobilized on mica. Analysis of low magnification AFM images (Fig. S7) using NIH ImageJ software indicates that the 1DrDO prepared avarage 12 ±4 (*N*=53) microns long. It is possible that in solution these 1DrDO are extremely long because of the strong interactions associated with the sticky end systems[22] used in the formation of these 1D extended origami structures. However short structures are observed on mica due both to deformation of the edge caused by potential local twist and curvature[17] and to structure disrupting flow associated forces accompanying sample preparation. High resolution AFM (Fig 3b) and line profile analysis (Fig. 3c) reflects the periodic pitch of the window landmarks. The same immobilized 1DrDO sample was subsequently incubated with SA. Figure 3d shows a ~4.3μm long 1DrDO (44 srDOs attached together) successfully modified with 88 SAs with ~44±3nm (*N*=134) spacing and ~96±3nm (*N*=140) pitch (Fig. 3f). Figure 3g provides an AFM image of 1DrDO after modification with SA-QDs to yield arrays of QDs (sQD-1DrDO). As in the previous case, the origami was immobilized on mica before incubation with SA-QD's. From the high-resolution AFM image shown in Fig. 3h, it is clear that all address sites are occupied. The line profile (Fig. 3i) demonstrates occupancy of the majority of locations by SA-QDs, however some locations are labeled with SA only, presumably because the QD solution contains some SA which has dissociated from the QDs. Fig. S11 shows the histogram of SA and SA-QDs height distribution on origami chain. After modification and rinsing, the sample background (mica) appears

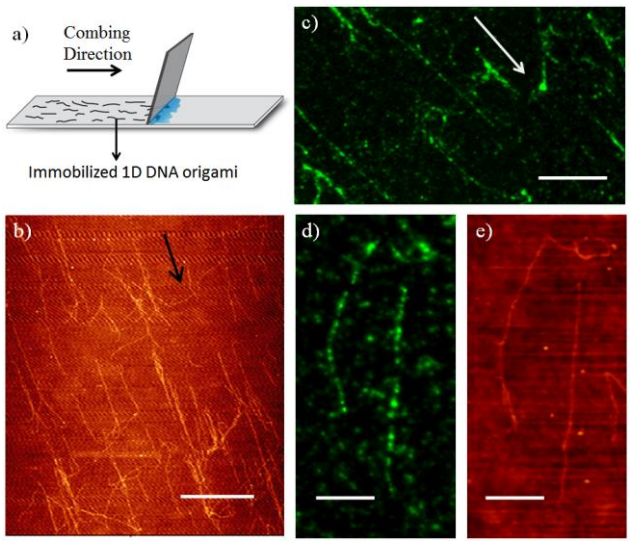

Figure 4. a) Schematic illustration a) presents the combing method for aligning sQD-1DrDO constructs on AP-glass; b) and c) large area AFM and FM view of sQD-1DrDO on AP-glass; arrow indicates the combing direction, Scale bar 10μm; d) and e) are AFM and FM images of the same region of the sample; Scale bar 5μm

to be free of extra SA (Fig. 3d); however, unattached SA-QDs are observed on the mica in Fig. 3g. It is possible that SA-QDs have a higher binding affinity to mica than SA, because the QDs have more protein to bind them to the surface. Quantitative analysis of the SA and SA-QD modification of the 1DrDO constructs was performed and the results are summarized in ESI Table 1. While 96% (*N*=307) of SA were successfully addressed to their sites on 1DrDO, the apparent rate is significantly lower for SA-QD labeling (71%, *N*=302).

Alignment of sQD-1DrDO constructs:

The molecular combing method[18] was applied to orient the sQD-1DrDO constracts on AP-glass along one direction as illustrated in Fig. 4a. The two main reasons for our focus on this method of "soft" manipulation of single 1DrDO molecules is first to determine the stability of the linkage in an orienting flow and secondly to generate aligned platforms for the analysis of the fluorescent properties of multiple copies in an array. These experiments introduce the use of the moleculer combing method for origami alignment and immobilization. Low magnification AFM (Fig. 4b) and fluorescence microscopy (FM) imaging (Fig. 4c) indicates that sQD-1DrDO constructs were succesfully aligned and immobilized on AP-glass coverslips. While the majority of the extended complexes are parallel, some of the 1DrDO were twisted (ESI Fig. S7c) and many were cross connected or entangled. Additionally, during the combing process, the orgami may anchor on the AP-glass at some point other than an end, resulting in the formation of a chevron shaped structure. Finally, any origami which is not immediately immobilized during combing can "relax" and acquire a different direction of immobilozation.[19] These long, threadlike constructs are almost certainly entangled in solution. Histogram of the origami chain alignment in ESI Fig. S8 indicates 77% (*N*=58) origami chains were immobilized along the combing direction. In order to observe the same molecules using both AFM and FM, indexed coverslips were used for locating the same region. Figure 4d and 4e presents an example of this kind of parallel analysis. The topography AFM image shows linear features on the AP-glass, which FM imaging confirms as QD fluorescence emission, verifying the identity of these long parallel lines as QD labeled 1DrDO constructs. The light microscopy image presented in ESI Fig. S9a shows the indexed AP-glass, the AFM tip position and the combing direction. The direction of the 1DrDO is consistent with the combing direction shown in the image in ESI Fig. S9b. Because the majority of even a captured 1DrDO construct would be freely diffusing, unconstrained in the buffer solution phase during combing, spiral or helical twisting can occur, resulting in twisted structures as seen in the high resolution AFM image shown in ESI Fig. S9c. Eliminating this twisting may prove to be challenging for long structures.

Conclusions

In summary, we have developed a rapid method to address SA and SA-QDs to selected sites on single and one dimensional origami constructs with useful yields. The SA labeling yield was ~99% when utilizing three biotins per binding location, while the apparent SA-QD labeling yield was significantly lower, ~77%. One major artifact, adventitious SA impurities in the QDot preparations may explain the majority of this loss of fidelity. In addition, each origami subunit within the 1D origami array was successfully labeled with these bio-conjugates at specific separations ~44±3nm with ~96±3nm pitch. The 1D constructs can withstand the molecular combing process, enabling their alignment before immobilization. These results indicate a promising future path to align semiconductor or metallic particles at specific separations and orientations using large DNA nanostructures, readily bridging the nanometer to micron size domains. Extension of this work in our lab is directed toward development of opto-electronic and electrochemical sensors.

Author would like to acknowledge the following grants for support to this research, ARO awards: W911NF-08-1-0109, W911NF-09-1-0218, W911NF-11-1-0024 and NSF Cooperative Agreement Number EPS-1003907.

Notes and references

1. N. C. Seeman, *Annual Review of Biochemistry*, 2010, **79**, 65-87.
2. N. C. Seeman and N. R. Kallenbach, *Biophys J*, 1983, **44**, 201-209.
3. N. C. Seeman, *Nature*, 2003, **421**, 427-431.
4. P. W. Rothemund, *Nature*, 2006, **440**, 297-302.
5. R. D. Barish, R. Schulman, P. W. Rothemund and E. Winfree, *Proc Natl Acad Sci U S A*, 2009, **106**, 6054-6059.
6. N. C. Seeman, *Mol Biotechnol*, 2007, **37**, 246-257.
7. K. Sarveswaran, W. Hu, P. W. Huber, G. H. Bernstein and M. Lieberman, *Langmuir*, 2006, **22**, 11279-11283.
8. W. M. Shih, J. D. Quispe and G. F. Joyce, *Nature*, 2004, **427**, 618-621.
9. W. Liu, H. Zhong, R. Wang and N. C. Seeman, *Angew Chem Int Ed Engl*, 2011, **50**, 264-267.
10. M. Endo, T. Sugita, Y. Katsuda, K. Hidaka and H. Sugiyama, *Chemistry*, 2010, **16**, 5362-5368.
11. K. Keren, R. S. Berman, E. Buchstab, U. Sivan and E. Braun, *Science*, 2003, **302**, 1380-1382.
12. A. C. Pearson, J. Liu, E. Pound, B. Uprety, A. T. Woolley, R. C. Davis and J. N. Harb, *The journal of physical chemistry. B*, 2012, **116**, 10551-10560.
13. H. T. Maune, S. P. Han, R. D. Barish, M. Bockrath, W. A. Iii, P. W. Rothemund and E. Winfree, *Nat Nanotechnol*, 2010, **5**, 61-66.
14. Z. Li, M. Liu, L. Wang, J. Nangreave, H. Yan and Y. Liu, *J Am Chem Soc*, 2010, **132**, 13545-13552.
15. F. Mathieu, S. Liao, J. Kopatsch, T. Wang, C. Mao and N. C. Seeman, *Nano Lett*, 2005, **5**, 661-665.
16. K. N. Kim, K. Sarveswaran, L. Mark and M. Lieberman, *Soft Matter*, 2011, **7**, 4636-4643.
17. S. Woo and P. W. K. Rothemund, *Nat Chem*, 2011, **3**, 620-627.
18. A. Bensimon, A. Simon, A. Chiffaudel, V. Croquette, F. Heslot and D. Bensimon, *Science*, 1994, **265**, 2096-2098.
19. T. Strick, J. Allemand, V. Croquette and D. Bensimon, *Progress in biophysics and molecular biology*, 2000, **74**, 115-140.
20. W. A. Hendrickson, A. Pahler, J. L. Smith, Y. Satow, E. A. Merritt and R. P. Phizackerley, *Proc Natl Acad Sci USA*, 1989, **86**, 2190-2194.
21. A. P. Eskelinen, A. Kuzyk, T. K. Kaltiaisenaho, M. Y. Timmermans, A. G. Nasibulin, E. I. Kauppinen and P. Torma, *Small*, 2011, **7**, 746-750.
22. J. Nangreave, H. Yan and Y. Liu, *Biophys J*, 2009, **97**, 563-571.

Table of Contents artwork

Demonstrate high yield biomolecule or conjugate assembly onto 1D DNA origami arrays and macroscopic alignment of the arrays via combing.